Journal of chemical & engineering data

Article

pubs.acs.org/jced

Diffusion Coefficients of CO_2 and N_2 in Water at Temperatures between 298.15 K and 423.15 K at Pressures up to 45 MPa

Shane P. Cadogan, Geoffrey C. Maitland, and J. P. Martin Trusler*

Qatar Carbonates and Carbon Storage Research Centre, Department of Chemical Engineering, Imperial College London, South Kensington Campus, London SW7 2AZ, United Kingdom

ABSTRACT: We report measurements of the diffusion coefficients of CO_2 and N_2 in pure water at temperatures between (298.15 and 423.15) K and pressures between (15 and 45) MPa. The measurements were made by the Taylor dispersion method and have a standard relative uncertainty of 2.3 %. The results were found to be essentially independent of pressure over the range investigated and a simple relation, based on the Stokes−Einstein equation, is proposed to correlate the experimental data. Some experimental difficulties arising in the measurement of the diffusivities of slightly soluble acid-gas solutes such as CO_2 in water are also discussed.

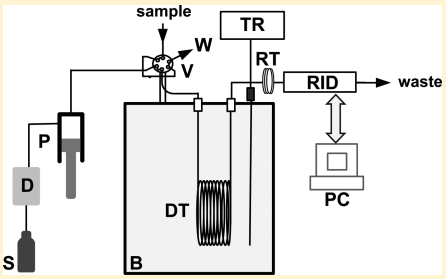

1. INTRODUCTION

The transport properties for (CO_2 + brine) systems are of special interest in the field of carbon capture, utilization, and sequestration (CCUS). Of the various sequestration sinks being considered, saline aquifers are believed to have the greatest capacity for storing CO_2 worldwide. However, the thermophysical properties of mixtures relevant to these systems are still subject to uncertainty, and diffusion coefficients, the subject of this investigation, are among the least-well studied.[1,2]

Diffusion processes in multicomponent mixtures are described by standard flow equations involving, in principle, a $N \times N$ diffusion matrix, where $N + 1$ is the number of species. Additionally, the elements of the diffusion matrix are generally dependent upon composition, as well as temperature and pressure. In the case of CO_2 diffusion in brine, it may be useful to approximate the brine itself as a pseudo-one-component solvent and, noting that CO_2 is only sparingly soluble, to treat the resulting single mutual diffusion coefficient as independent of CO_2 concentration in the accessible limited range. In that approximation, the dispersion of the sequestered CO_2 in the brine-saturated heterogeneous porous media can be described as a function of the Peclet number,[3] *Pe*. The Peclet number is defined as the ratio of advection, $L{\cdot}v$, to the mutual diffusion coefficient, D, where L is a characteristic length and v is the appropriate average velocity.[4] For flow in a capillary of radius R, $Pe = 2Rv/D$ and v is the linear flow velocity averaged over the cross-section of the capillary. According to Sahimi,[5] diffusion is the dominant mechanism of dispersion in porous media when $Pe \leq 5$, and is significant up to $Pe \approx 300$. This corresponds to fluid velocities on the order of $cm{\cdot}s^{-1}$ in microporous media with R of order 10^{-6} m and D of order 10^{-9} $m^2{\cdot}s^{-1}$. Except close to points of injection, the *Pe* is typically low and the transport of solute molecules is strongly influenced by diffusion. Reliable knowledge of the diffusion coefficients, and other thermophysical properties, in systems comprising carbon dioxide, brines, and hydrocarbons is therefore necessary for the rational design, control, and optimization of CCUS processes.

The Taylor dispersion method has been used widely in the last 30 years for the measurement of diffusion coefficients. This technique exploits the dispersion experienced by a solute plug when injected into a laminar flow. Axial dispersion, primarily resulting from the parabolic flow profile, acts to spread the solute pulse out longitudinally, while radial diffusion acts to keep the pulse confined. The combined result of these two phenomena is to produce an essentially Gaussian distribution after a sufficient amount of time has passed for the flow to become fully developed. The dispersion coefficient which described this Gaussian distribution has been related to the mutual diffusion coefficient by Taylor[6] and Aris.[7] Several authors have published widely on this technique, in particular Leaist[8,9] has considered multicomponent systems, and Funazukuri et al.[10] studied supercritical systems. There has also been extensive work carried out to gauge the influence of practical parameters on the accuracy of the technique, for example, the work of Alizadeh et al.[11]

Despite the frequent use of Taylor dispersion as a method for measuring diffusion coefficients, only a few workers have employed this technique to measure the diffusion coefficients for gases dissolved in liquids. Ferrell and Himmleblau[12] have used the Taylor dispersion method to measure the tracer diffusion coefficients of CO_2, and N_2 in water, as did Snijder et al.[13] and Frank et al.[14] for CO_2 in water as part of a study of the diffusion of various gases in nonaqueous solvents. Additionally, Han and Bartels[15] have reported on diffusion coefficients of O_2 in water and D_2O, and Hamborg et al. have used the Taylor dispersion technique for N_2O in aqueous piperazine.[16]

Received: November 20, 2013
Accepted: December 27, 2013
Published: January 9, 2014

The main aim of the present work was to extend previous measurements of the tracer diffusion coefficient of CO_2 in pure H_2O to high pressures and high temperatures. The Taylor dispersion apparatus described previously[17] was used for this purpose, and several issues regarding the accurate determination of diffusion coefficients for gases in liquids are highlighted in this paper. The effect of dissolved salts is a topic for future work.

2. EXPERIMENTAL SECTION

2.1. Methodology. Figure 1 is a schematic diagram of the Taylor dispersion apparatus used in this work. With the exception of the solution preparation system, the apparatus was as described by Secuianu et al.[17] It comprised four modules: a solvent delivery system with a solution injection valve; a solution preparation vessel; a thermostatic oil bath housing the diffusion capillary; and a differential refractive-index detector. The solution preparation vessel, fabricated from titanium, had an internal volume of 100 mL and was fitted with a PTFE-coated magnetic stirrer bar. This vessel was used, first, to degas a quantity of solvent and then to saturate it with gas at ambient temperature and a pressure of up to 0.7 MPa. Prior to an injection, the gas-saturated solution was passed under pressure, via a dip tube in the vessel, through a 5 μL sample loop on the 6-port injection valve, and via a back pressure regulator to waste. This back pressure regulator served to prevent the solute from coming out of solution prior to injection into the diffusion column. A syringe pump (Teledyne ISCO model 100DM) was used to provide a continuous flow of solvent through, in turn, the 6-port injection valve, a coiled diffusion column, housed in a thermostatic oil bath (Fluke model 6022), a PEEK-reinforced-silica restriction tube, a differential refractive index detector (RID, Agilent 1200 series), and finally a second back-pressure regulator. The purpose of the restriction tube was to permit high pressures in the diffusion column, up to 50 MPa, while allowing the refractive index detector to operate at a low pressure (typically 0.45 MPa) set by the back-pressure regulator. Several restriction tubes were used in this work to allow measurements to be performed at different pressures and flow rates. The syringe pump was operated in flow-control mode at various flow rates consistent with the desired operating pressure and the avoidance of secondary flow. The pressure was measured in the pump head, and the calculated pressure drop across the diffusion tube was found to be negligible. With the exception of the restriction tubes, all the tubing prior to the detector was made from Hastelloy C-276. The diffusion column had a length of 4.518 m, as measured with an ordinary tape measure, and an internal radius of 0.5398 mm, as determined gravimetrically. Interconnecting tubing outside the thermostatic oil bath was of small diameter to minimize the dispersion in these sections.[17]

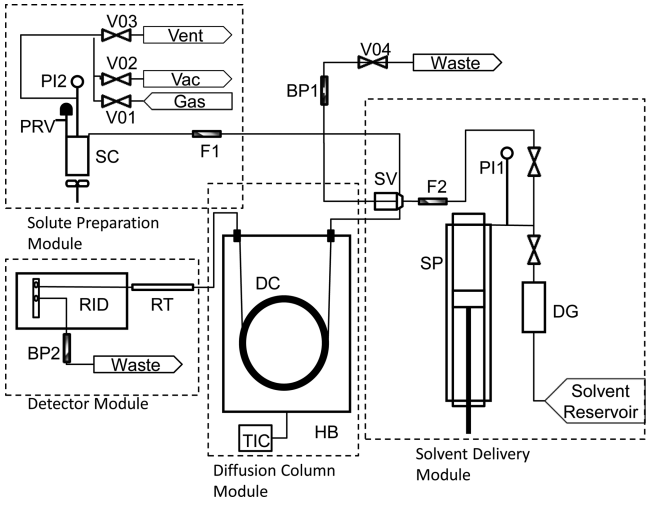

Figure 1. Schematic of the Taylor dispersion apparatus: DG, vacuum degasser; SP, syringe pump; PI1 and PI2, pressure transducers; F1 and F2, filters; SV, sample valve; DC, diffusion column; HB, thermostatic oil bath; TIC, temperature controller; RT, restriction tube; RID, refractive index detector; BP1 and BP2, back pressure valves; SC, saturation chamber; PRV; proportional relief valve; V01, V02, and V03, gas and vacuum valves; V04; solution outlet valve.

The temperature of the oil bath was measured with a secondary-standard platinum resistance thermometer (Fluke Hart Scientific model 5615) and readout unit (Fluke Hart Scientific, model 1502A). The thermometer was calibrated on ITS-90 at the temperature of the triple point of water and by comparison in a constant temperature bath with a standard platinum resistance thermometer at nominal temperatures of (323, 373, 423, and 473) K. The standard uncertainty of the temperature measurements was 0.01 K. The solvent delivery pressure was measured at the outflow of the pump by means of the pressure transducer integrated into the pump. According to the manufacturer, the relative uncertainty of the pressure was 0.5 % of the reading, and we take this figure to be the expanded relative uncertainty with a coverage factor of 2.

The solvent used in this study was pure deionized water with an electrical resistivity of >18.2 MΩ·cm at T = 298.15 K. The solvent was degassed before entering the pump via an in-line degasser (Knauer model A5328). CO_2 and N_2, both of 99.995% purity, were supplied by BOC. The pump was maintained at T = 293 K by passing water from a chiller (Huber Minichiller) through a jacket around the syringe. The chiller also supplied a flow of water to a coldfinger inserted in the thermostatic bath to permit operation at temperatures below about 313 K at which temperature natural heat loss was insufficient.

Solutions of the gas under study in pure water were typically prepared at a pressure of 0.7 MPa, giving a solute concentration of about 0.2 mol·L^{-1} for CO_2 and 0.005 mol·L^{-1} for N_2.[18,19] Once thermal equilibrium was established in the thermostatic bath and steady-state flow was established, as evidenced by a constant pressure upstream of the column, a series of solution injections were made. Typically, 4 to 6 repeat measurements were made at each temperature and pressure.

The differential refractive index signal $s(t)$ was analyzed in terms of the relation

$$s(t) = a + bt + \alpha c(t) \quad (1)$$

where a and b are baseline coefficients, t is time, c is molar solute concentration, and $\alpha = (\partial s/\partial c)_{T,p}$ is the sensitivity of the detector (assumed constant). The concentration profile was given by the relation of Aris[7]

$$c(t) = \{n/(\pi R^2\sqrt{4\pi Kt})\}\exp[-(L - vt)^2/4Kt] \quad (2)$$

Here, n is the amount of solute injected, R is the radius, and L is the effective length of the column, v is the linear flow rate of solvent averaged over the cross-section of the tube, and K is the dispersion coefficient, normally related to the diffusion coefficient D by

$$K = D + (R^2v^2/48D) \quad (3)$$

dx.doi.org/10.1021/je401008s | J. Chem. Eng. Data 2014, 59, 519−525

The effective length is given by

$$L = L_c + (D/D_0) \sum_{i=1}^{3} (R_i/R_c)^4 L_i \quad (4)$$

where D is the diffusion coefficient at the column temperature, D_0 is the diffusion coefficient at the ambient temperature, and subscript i = 1, 2, 3, c for the inlet, outlet, RID, and column sections, respectively. This correction is small, with L typically being less than 1.5 % greater than L_c.

The analysis consisted of adjusting the baseline coefficients, the diffusion coefficient, and the product $n\alpha$ so as to best fit the experimental signal.

In this work, the sensitivity coefficient α was estimated for CO_2 in water by flowing solution directly through the RID, which was operated at T = 308.15 K. The composition of the solution was calculated from the measured temperature and pressure in the saturation chamber using the solubility model of Duan and Sun.[18] This gave $\alpha = -7.4 \times 10^{-4}$ L·mol^{-1}; the negative sign indicates that the refractive index decreases with increasing concentration of solute as also observed by Watson.[20] For N_2 in water, α was calculated from the molar refractivities and partial molar volume of N_2 given by Harvey et al.[19] and was found to be -4.0×10^{-3} L·mol^{-1}. The sensitivity is not needed in the analysis to determine D but it was used to verify that the peak concentration of solute was below the solubility limit at the temperature and pressure prevailing in the detector. The low concentrations of CO_2 mean that it was effectively the tracer diffusion coefficient that was measured in these experiments.

2.2. Selection of Optimal Operating Conditions. The optimal operating conditions for a Taylor Dispersion apparatus have been discussed by several authors. The main criteria are that the flow should be laminar and that secondary flow induced by coiling of the capillary should be negligible. The second criterion is often associated in the literature with an upper limit on the product De^2Sc, where $De = Re(R/R_{coil})^{1/2}$ is the Dean number, $Sc = \eta/(\rho D)$ is the Schmidt number, $Re = (2R\nu\rho/\eta)$ is the Reynolds number, R_{coil} is the coil radius, η is the solvent viscosity, and ρ is the solvent density. In our previous work, with the same apparatus, the system (KCl + H_2O) was studied at flow rates such that De^2Sc was less than about 20 and the measured signals $s(t)$ conformed closely to the working equation. In the present work with gaseous solutes it proved necessary to reappraise the optimal flow-rate and to consider corrections to eq 3 for the effects of secondary flow. Such corrections have been developed by Erdogan and Chatwin[21] and by Nunge et al.;[22] the latter's formulation is discussed further below.

Figure 2 is an example of the signal $s(t)$ corresponding to an injection of N_2(aq) into pure water flowing at 0.08 mL·min^{-1} at a pressure of 26.6 MPa with a column temperature of 423.15 K. Also shown are the deviations of $s(t)$ from the fit with eqs 1 and 2. The experimental data are seen to conform closely to the working equation with deviations not worse than about ± 1 % of the peak signal. In this case, $De^2Sc \approx 5$.

In contrast to the situation with nitrogen, injections of CO_2(aq) resulted in an anomalous peak shape at comparable flow rates (roughly ≤0.12 mL·min^{-1}) and $T \geq$ 348.15 K. Figure 3 is an example of such behavior and shows a pronounced prepeak of reverse polarity. Despite exhaustive investigations, the origin of this prepeak, which has a transit time up to 60 s faster than the mean liquid residence time, has not been

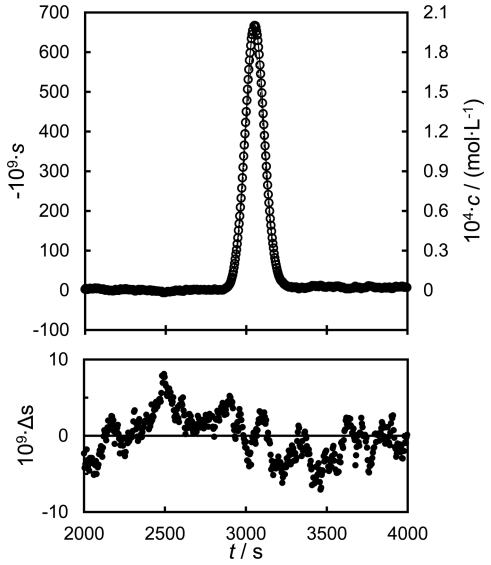

Figure 2. (top) Dispersion curve $s(t)$ for N_2 in water at T = 423 K, p = 26.6 MPa, and a flow rate of 0.08 mL·min^{-1}: ○, refractive index signal; ———, Aris model, eqs 1 to 3 fitted to the experimental data. (bottom) Deviations Δs between the experimental data and the fitted model.

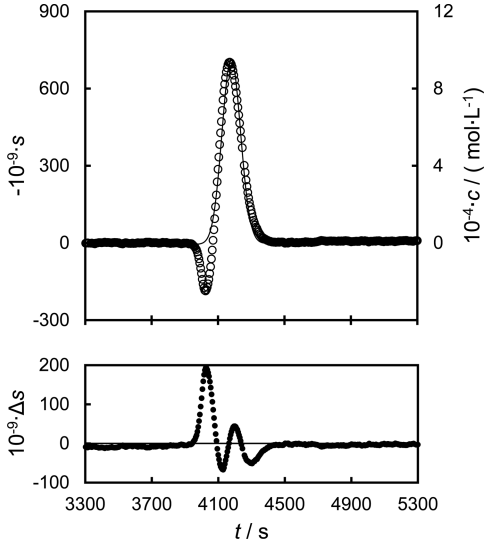

Figure 3. (top) Dispersion curve $s(t)$ for CO_2 in water at T = 423 K, p = 9.9 MPa, and a flow rate of 0.03 mL·min^{-1}: ○, refractive index signal; ———, Aris model, eqs 1 to 3 fitted to the experimental data. (bottom) Deviations Δs between the experimental data and the fitted model.

determined. The fact that H^+ and HCO_3^- ions, formed by the hydrolysis of CO_2, would be present is an obvious factor distinguishing this case from that of nitrogen. Since the fraction ε of the CO_2 hydrolyzed at equilibrium is approximately $(K_1/c)^{1/2}$, where c is the concentration of dissolved CO_2 and K_1 is the equilibrium constant of the hydrolysis reaction in concentration units, the ionic species are expected to be relatively more prevalent toward the edges of the main peak. At the detector temperature of 308.15 K, $K_1 = 4.9 \cdot 10^{-7}$ mol·L^{-1},[23] so for the case illustrated in Figure 3 $\varepsilon \approx 2.2$ % at the peak concentration and about 7 % at one-tenth of the peak concentration. Although ε is quite small, the sensitivity of the RID to $H^+ + HCO_3^-$, estimated by combining refractive index

dx.doi.org/10.1021/je401008s | J. Chem. Eng. Data 2014, 59, 519−525

data of aqueous $NaHCO_3$, HCl, and NaCl,[24] is approximately 10 times that to molecular CO_2 and of the opposite polarity. Thus the presence of ions should make a significant contribution to the RID signal in opposition to that of molecular CO_2. Consistent with a hydrolysis mechanism, it was also found that the ratio of the prepeak to the main peak increased in magnitude when more dilute solutions of CO_2 were injected. However, we could find no reason why the products of hydrolysis would accumulate on the leading edge instead of being everywhere in local thermodynamic equilibrium with CO_2. Check runs in which the mobile phase was acidified with HCl to a pH of about 4 to inhibit hydrolysis were performed; however, the prepeaks were still present. Thus the evidence does not prove a clear connection with hydrolysis. Tests for possible interactions of the CO_2 with the wall material were also inconclusive: with stainless steel the situation was unchanged but with a PEEK tube the CO_2 was entirely absorbed. The possibility that the CO_2 was coming out of solution in the detector was eliminated by comparing the measured concentration with the solubility limit and also by looking for bubbles in the solution flowing between the RID and the back-pressure regulator at the outlet (transparent tubing was installed for this purpose). It was observed that, with solvent flowing continuously, the height of the prepeak (relative to the main peak) decreased in magnitude over a series of solute injections; however, it increased again after a period without injections. It was also found that the prepeaks were greatly diminished when the flow rate was increased.

To suppress the anomalous prepeak while limiting the effects of secondary-flow effects, the measurements for CO_2 in water were made at flow rates of (0.305 to 0.325) mL·min^{-1}, corresponding to $80 < De^2Sc < 100$. Figure 4 shows and example of the RID signal measured for CO_2 in water at T = 423.15 K and a flow rate of 0.325 mL·min^{-1}, under which conditions no prepeak is evident, and the data conform to eqs 1 and 2. The amount of solute eluting, obtained from the area under the peak, was found to agree within about 15% with the calculated amount injected, based on the solubility model, the temperature, and pressure in the solution preparation vessel and the nominal volume of the sample loop. We note that the value of D determined from the anomalous data shown in Figure 3 was 20 % higher than the value obtained from the "normal" dispersion curve shown in Figure 4. Although we cannot rule out the persistence of some systematic errors in our final results, we expect these to be much smaller than the differences in the values of D obtained with low and high flow rates. At the flow rates necessary to achieve acceptable peak shapes, secondary flow effects are still small but not negligible. To account for this, eq 3 for the dispersion coefficient K was replaced by the more general expression derived by Nunge et al.:[22]

$$K = \left[D + \frac{R^2v^2}{48D}\right] + (Pe^2D)(De^2Sc)^2 \times \left[\frac{1}{40 \times 576^2}\left\{\frac{-2569}{15840} + \frac{109}{43200Sc^2}\right\} + \frac{1}{72 \times 576\mathrm{Re}^2}\left\{\frac{31}{60Sc} - \frac{25497}{13440Sc^2}\right\} + \frac{1}{\mathrm{Re}^4Sc^2}\left\{\frac{419}{11520} + \frac{1}{4}\left(\frac{1}{Pe^2} + \frac{1}{192}\right)\right\}\right] \quad (5)$$

The use of eq 5 in place of eq 3 to calculate D from K implies a relative correction of between −1.4% and −1.7% in the present work. We note that under typical operating conditions for a Taylor Dispersion experiment, $Sc \gg 1$, $10^\circ \leq Re \leq 10^2$, and $K \gg D$, so that eq 5 reduces to the following simple expression in which the correction for secondary flow is directly proportional to $(De^2Sc)^2$:

$$K \approx \left(\frac{R^2v^2}{48D}\right)\left[1 - \left(\frac{De^2Sc}{653}\right)^2\right] \quad (6)$$

Having determined the optimal operating conditions, measurements for CO_2 in water, as well as N_2 in water, were made over the temperature range (298 to 423) K at pressures up to 45 MPa. In these measurements, dispersion curves like those seen in Figure 4 were always observed and enable the diffusion coefficient to be extracted with an estimated standard relative uncertainty of 2.3 %.

2.3. Materials. Ultrapure deionized water with electrical resistivity > 18 MΩ·cm was obtained from a Millipore system (Direct-Q, Millipore UK Ltd.). The nitrogen and carbon dioxide were supplied by BOC with claimed mole-fraction purities of 0.99998 and 0.99995, respectively.

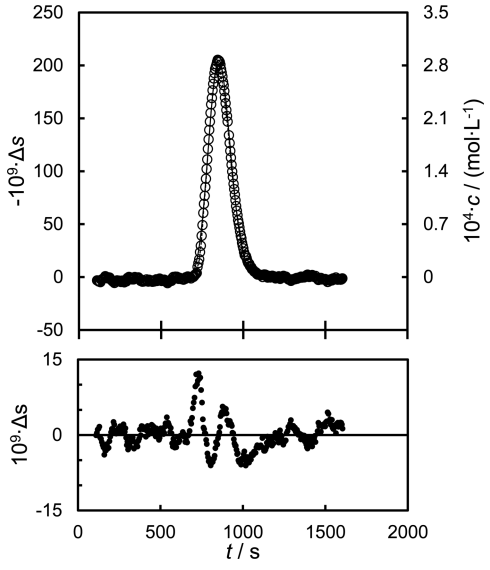

Figure 4. (top) Dispersion curve $s(t)$ for CO_2 in water at T = 423 K, p = 39 MPa, and a flow rate of 0.325 mL·min^{-1}: ○, refractive index signal; ———, Aris model, eqs 1 to 3 fitted to the experimental data. (bottom) Deviations Δs between the experimental data and the fitted model.

3. RESULTS

The values of the diffusion coefficient for N_2 in water over the temperature range (298 to 423) K and pressure range (12 to 46) MPa are given in Table 1. The mean linear flow speed v, the maximum sum of squared deviation of $s(t)$ from the fitted Aris model for an accepted peak in an experiment, $10^2\sigma_{s,\max}$, and standard deviation of D, σ_D, over N injections are also tabulated. The dimensions of the restriction tube used for all these experiments were 25 μm (inner diameter) × 250 mm (length). The results are plotted as a function of temperature in Figure 5.

dx.doi.org/10.1021/je401008s | J. Chem. Eng. Data 2014, 59, 519−525

Table 1. Diffusion Coefficients D and Standard Deviations σ_D for N_2 in Water at Temperatures T and Pressure p Determined from N Repeated Injections at Mean Solvent Flow Speed v, Together with the Maximum Relative Standard Deviation $(\sigma_s/s_{max})_{max}$ of the RID Signal $s(t)$, Where s_{max} Is the Maximum Value of s[a]

T	p	v	D			
K	MPa	m·s^{-1}	10^{-9} m^2·s^{-1}	N	$10^2(\sigma_D/D)$	$10^2(\sigma_s/s_{max})_{max}$
298	12.0	0.035	1.989	7	0.6	0.8
298	25.0	0.075	2.000	3	0.6	1.1
298	44.6	0.140	1.979	4	5.7	1.9
323	14.6	0.045	3.278	4	0.6	0.9
323	25.1	0.075	3.468	3	1.0	0.9
323	45.0	0.140	3.203	5	3.0	1.7
373	14.8	0.035	6.619	6	2.7	0.6
373	45.0	0.115	6.425	6	3.3	1.5
423	26.9	0.080	10.73	4	0.7	0.6
423	45.9	0.140	10.42	5	1.6	0.6

[a]Standard uncertainties are $u(T)$ = 0.01 K, $u(p)$ = 0.0025·p and $u(D)$ = 0.023D.

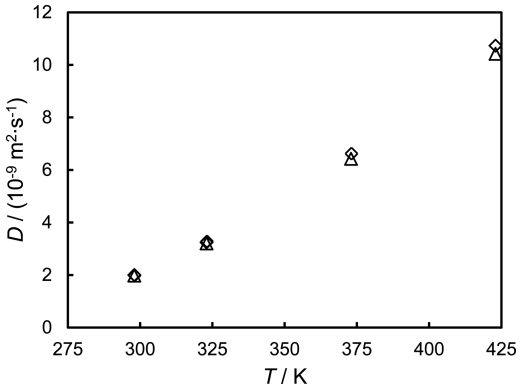

Figure 5. Diffusion coefficients D of N_2 in water as a function of temperature T: ◇, p = (12.0 to 14.8) MPa; □, p = (25.0 to 26.9) MPa; △, p = (44.6 to 45.9) MPa.

The measured diffusion coefficients for CO_2 in water over the range (298 to 423) K and (14 to 50) MPa are given in Table 2, together with the mean linear flow speed, the maximum sum of squared deviation of the fitted $s(t)$ for an accepted peak in an experiment, and the standard deviation of D over N injections. The results are plotted as a function of temperature in Figure 6.

The standard relative uncertainty associated with these measurements was calculated from the following equation:

$$u_r^2(D) = u_r^2(K) + 4u_r^2(R) + 4u_r^2(v) + [(p/D)(\partial D/\partial p)u_r(p)]^2 + [D^{-1}(\partial D/\partial T)u(T)]^2 \quad (7)$$

where $u_r(X)$ denotes standard relative uncertainty and $u(X)$ standard uncertainty of variable X. The standard relative uncertainties appearing on the right of eq 7 were $u_r(K)$ = 2 %, estimated from the repeatability of the dispersion measurements, $u_r(R)$ = 0.2 %, $u_r(v)$ = 0.5 %, and $u_r(p)$ = 0.25 %, while the standard uncertainty of temperature was 0.01 K. This led to $u_r(D)$ = 2.3 % for both systems investigated. This figure is dominated by the repeatability of K; the uncertainties of T and p have negligible influence.

Table 2. Diffusion Coefficients D and Standard Deviations σ_D for CO_2 in Water at Temperatures T and Pressure p Determined from N Repeated Injections at Mean Solvent Flow Speed v, Together with the Maximum Relative Standard Deviation $(\sigma_s/s_{max})_{max}$ of the RID Signal $s(t)$, Where s_{max} Is the Maximum Value of s[a]

T	p	v	D			
K	MPa	m·s^{-1}	10^{-9} m^2·s^{-1}	N	$10^2(\sigma_D/D)$	$10^2(\sigma_s/s_{max})_{max}$
298	14.0	0.305[b]	2.233	4	1.8	1.3
298	31.6	0.305[c]	2.256	5	3.2	1.8
298	47.7	0.305[d]	2.218	5	1.4	0.8
323	14.2	0.315[b]	3.643	4	1.4	1.4
323	31.8	0.315[c]	3.718	6	1.6	2.0
323	48.6	0.315[d]	3.938	4	2.3	2.4
348	14.9	0.325[b]	5.391	4	1.3	1.8
348	31.8	0.325[c]	5.306	5	1.8	2.6
348	49.3	0.325[d]	5.366	6	2.0	2.3
373	14.9	0.325[b]	7.416	5	0.8	1.8
373	31.0	0.325[c]	7.521	5	4.0	2.3
373	48.5	0.325[d]	7.681	5	1.6	2.8
398	14.3	0.325[b]	9.949	5	3.3	1.7
398	30.9	0.325[c]	10.06	4	1.6	2.3
398	48.0	0.325[d]	10.17	6	3.1	2.3
423	14.3	0.325[b]	12.33	4	1.7	1.3
423	48.0	0.325[d]	12.21	5	1.6	2.4

[a]Standard uncertainties are $u(T)$ = 0.01 K, $u(p)$ = 0.0025·p and $u(D)$ = 0.023D. [b]50 μm i.d. × 500 mm long restriction tube used. [c]25 μm i.d. × 50 mm long restriction tube used. [d]25 μm i.d. × 100 mm long restriction tube used.

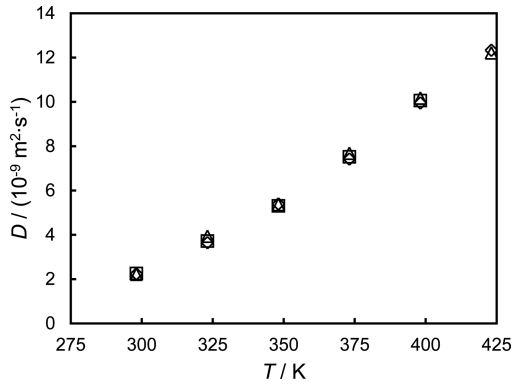

Figure 6. Diffusion coefficients D for CO_2 in water as a function of temperature T: ◇, p = (14.0 to 14.9) MPa; □, p = (30.9 to 31.8) MPa; △, p = (47.7 to 49.3) MPa.

4. DISCUSSION

While the reproducibility found in the present experiments was somewhat lower than obtained by Secuianu et al.[17] for the (KCl + H_2O) system using the same equipment, the results obtained were generally consistent within ± 3 % at a given state point. An important observation for both systems is that the diffusion coefficients are not significantly dependent upon pressure in the ranges of p and T investigated. Rutte has discussed the use of a modified Stokes−Einstein equation to describe the temperature dependence of the diffusion coefficients of gases in liquids:[25]

$$D = \{k_B T/(n_{SE}\pi\eta a)\} \quad (7a)$$

Here, k_B is Boltzmann's constant, T is temperature, n_{SE} is the Stokes−Einstein number, η is the solvent viscosity, and a is the

dx.doi.org/10.1021/je401008s | J. Chem. Eng. Data 2014, 59, 519−525

hydrodynamic radius of the solute. Typically, the hydrodynamic radius a is found to be a weak function of temperature and, in the present work, we correlate this term as follows:

$$a = a_{298}[1 + \alpha_a(T/\mathrm{K} - 298)] \quad (8)$$

The inclusion of a temperature dependence of the hydrodynamic radius is an alternative to introduction of an exponent for the solvent viscosity in eq 7 as has been proposed by other authors.[15] The influence of temperature on the hydrodynamic radius has been rationalized by Schultz and Solomon[26] and Krynicki et al.[27]

For consistency with previous work, we take the Stokes–Einstein number to be 4.

4.1. N_2 + H_2O System. The results of the present investigation are represented with a relative standard deviation of 2.1 % by eqs 7 and 8 with a_{298} = 190 pm and $\alpha_a = 2.2 \cdot 10^{-3}$. Figure 7 shows the present results and those of Ferrell and Himmleblau,[12] Wise and Houghton,[28] and Verhallen et al.[29] as deviation from this correlation. There is considerable disagreement between literature sources. Ferrell and Himmleblau[12] used the Taylor dispersion method at four different temperatures and reported results with relative standard deviations averaging 8 %. Their results are between (0 and 11) % higher than the present correlation, which is reasonable in the light of the claimed uncertainties. In contrast, Wise and Houghton[28] used a method based on the rate of bubble collapse, with a claimed relative uncertainty of 10 %, and report results that are (34 to 41) % higher than the present correlation. Verhallen et al.[29] used a method based on the permeability of gas through a stagnant layer of liquid in quasi-steady state, and claim a relative uncertainty of 5 %; their results are (14 to 22) % higher than the present correlation.

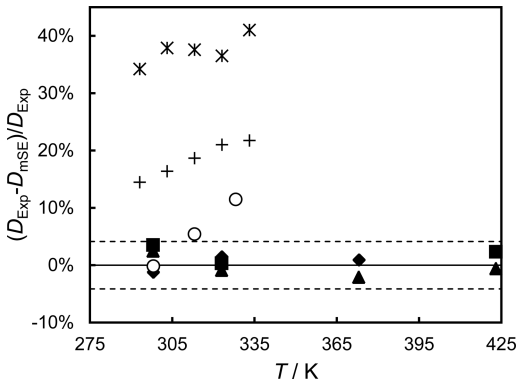

Figure 7. Deviations of experimental diffusion coefficients D_{Exp} from the values D_{SE} calculated from the modified Stokes–Einstein equation for N_2 in H_2O: ♦, this work at p = (14.0 and 14.9) MPa; ■, this work at p = (30.9 to 31.8) MPa; ▲, this work at p = (47.7 to 49.3) MPa; ○, Ferrell and Himmleblau;[12] +, Verhallen et al.;[29] ∗, Wise and Houghton;[28] ---, 95% confidence interval for the modified Stokes–Einstein correlation.

4.2. CO_2 + H_2O System. The results of the present investigation are represented with a relative standard deviation of 2.9 % by eqs 7 and 8 with a_{298} = 168 pm and $\alpha_a = 2.0 \cdot 10^{-3}$. The point at T = 323 K and p near 48 MPa appears to be an outlier but otherwise the results fall within ± 4 % of the correlation, which is reasonable in the light of the 2.3 % relative standard uncertainty. Figure 8 shows the present results and data from the literature[12,14,30−34] as deviation from this correlation. There is a considerable amount of scatter in the values reported in the literature; however most of the published data for D are somewhat below the correlation of our results. However, the values of D reported by Tamimi and Rinker,[33] who chose a wetted-sphere apparatus for their measurements, indicates a somewhat different trend. The majority of the values reported were determined by measuring the rate of absorption of CO_2 into a geometrically well-defined body of water.[30,32−34] The interpretation of these measurements relies on accurate knowledge of the solubility of the gas in the water, and errors in this quantity have a large influence on the value of D.

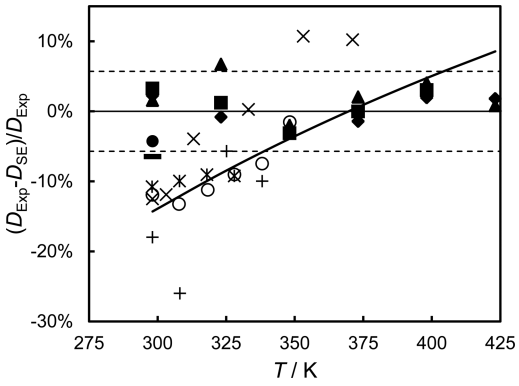

Figure 8. Deviations of experimental diffusion coefficients D_{Exp} from the values D_{SE} calculated from the modified Stokes–Einstein equation for CO_2 in H_2O: ♦, this work at p = (14.0 to 14.9) MPa; ■, this work at p = (30.9 to 31.8) MPa; ▲, this work at p = (47.7 to 49.3) MPa; ∗, Frank et al.;[14] ○, Thomas and Adams;[30] △, Clarke;[32] ×, Tamimi and Rinker;[33] +, Unver and Himmleblau;[34] □, Tse and Sandall;[35] ———, correlation of Thomas and Adams[30] as used by Grogan and Pinczewski;[31] ---, 95% confidence interval for the modified Stokes–Einstein correlation.

5. CONCLUSIONS

Despite the experimental difficulties encountered, diffusion coefficients for (N_2 + H_2O) and (CO_2 + H_2O) systems have been obtained over wide ranges of temperature and pressure with standard uncertainties of about 2.3 %. Correlations, based on the Stokes–Einstein equation, have been proposed for the diffusion coefficient of both N_2 and CO_2 in water as a function of temperature and solvent viscosity. The effect of pressure on the diffusion coefficient was found to be negligible in the ranges investigated. The non-Gaussian behavior observed at higher temperatures and low flow rates during measurements on the (CO_2 + H_2O) system remains unexplained.

■ AUTHOR INFORMATION

Corresponding Author

*E-mail: m.trusler@imperial.ac.uk.

Funding

We gratefully acknowledge the funding of QCCSRC provided jointly by Qatar Petroleum, Shell, and the Qatar Science & Technology Park.

Notes

The authors declare no competing financial interest.

■ ACKNOWLEDGMENTS

We are pleased to acknowledge useful discussions with Dr Catinca Secuianu.

REFERENCES

(1) Li, H.; Wilhelmsen, Ø.; Lv, Y.; Wang, W.; Yan, J. Viscosities, thermal conductivities and diffusion coefficients of CO_2 mixtures: Review of experimental data and theoretical models. *Int. J. Greenhouse Gas Control* **2011**, *5*, 1119−1139.

(2) Abu-Arabi, M. K.; Al-Jarrah, A. M.; El-Eideh, M.; Tamimi, A. Physical solubility and diffusivity of CO_2 in aqueous diethanolamine solutions. *J. Chem. Eng. Data* **2001**, *46*, 516−521.

(3) Bijeljic, B.; Blunt, M. J. Pore-scale modeling and continuous time random walk analysis of dispersion in porous media. *Water Resour. Res.* **2006**, *42*, W01202.

(4) Perkins, T.; Johnston, O. A review of diffusion and dispersion in porous media. *SPE J.* **1963**, *3*, 70−84.

(5) Sahimi, M. *Flow and Transport in Porous Media and Fractured Rock*; Wiley: Berlin, 1995.

(6) Taylor, G. Dispersion of soluble matter in solvent flowing slowly through a tube. *Proc. R. Soc. London, Ser. A.* **1953**, *219*, 186−203.

(7) Aris, R. On the dispersion of a solute in a fluid flowing through a tube. *Proc. R. Soc. London, Ser. A* **1956**, *235*, 67−77.

(8) Leaist, D. G. Ternary diffusion coefficients of 18-crown-6 ether−KCl−water by direct least-squares analysis of Taylor dispersion measurements. *J. Chem. Soc., Faraday Trans.* **1991**, *87*, 597−601.

(9) Callendar, R.; Leaist, D. G. Diffusion coefficients for binary, ternary, and polydisperse solutions from peak-width analysis of Taylor dispersion profiles. *J. Solution Chem.* **2006**, *35*, 353−379.

(10) Funazukuri, T.; Kong, C. Y.; Kagei, S. Binary diffusion coefficients in supercritical fluids: Recent progress in measurements and correlations for binary diffusion coefficients. *J. Supercrit. Fluids* **2006**, *38*, 201−210.

(11) Alizadeh, A.; De Castro, C. N.; Wakeham, W. The theory of the Taylor dispersion technique for liquid diffusivity measurements. *Int. J. Thermophys.* **1980**, *1*, 243−284.

(12) Ferrell, R. T.; Himmelblau, D. M. Diffusion coefficients of nitrogen and oxygen in water. *J. Chem. Eng. Data* **1967**, *12*, 111−115.

(13) Snijder, E. D.; te Riele, M. J.; Versteeg, G. F.; van Swaaij, W. P. Diffusion coefficients of CO, CO_2, N_2O, and N_2 in ethanol and toluene. *J. Chem. Eng. Data* **1995**, *40*, 37−39.

(14) Frank, M. J.; Kuipers, J. A.; van Swaaij, W. P. Diffusion coefficients and viscosities of CO_2 + H_2O, CO_2 + CH_3OH, NH_3 + H_2O, and NH_3 + CH_3OH liquid mixtures. *J. Chem. Eng. Data* **1996**, *41*, 297−302.

(15) Han, P.; Bartels, D. M. Temperature dependence of oxygen diffusion in H_2O and D_2O. *J. Phys. Chem.* **1996**, *100*, 5597−5602.

(16) Hamborg, E. S.; Derks, P. W.; Kersten, S. R.; Niederer, J. P.; Versteeg, G. F. Diffusion Coefficients of N_2O in Aqueous Piperazine Solutions Using the Taylor Dispersion Technique from (293 to 333) K and (0.3 to 1.4) mol·dm^{-3}. *J. Chem. Eng. Data* **2008**, *53*, 1462−1466.

(17) Secuianu, C.; Maitland, G. C.; Trusler, J. M.; Wakeham, W. A. Mutual diffusion coefficients of aqueous KCl at high pressures measured by the Taylor dispersion method. *J. Chem. Eng. Data* **2011**, *56*, 4840−4848.

(18) Duan, Z.; Sun, R. An improved model calculating CO_2 solubility in pure water and aqueous NaCl solutions from 273 to 533 K and from 0 to 2000 bar. *Chem. Geol.* **2003**, *193*, 257−271.

(19) Harvey, A.; Kaplan, S. G.; Burnett, J. Effect of dissolved air on the density and refractive index of water. *Int. J. Thermophys.* **2005**, *26*, 1495−1514.

(20) Watson, H. The refractive indices of aqueous solutions of H_2O^{18} and CO_2. *J. Am. Chem. Soc.* **1954**, *76*, 5884−5886.

(21) Erdogan, M. E.; Chatwin, P. The effects of curvature and buoyancy on the laminar dispersion of solute in a horizontal tube. *J. Fluid Mech.* **1967**, *29*, 465−484.

(22) Nunge, R.; Lin, T.; Gill, W. Laminar dispersion in curved tubes and channels. *J. Fluid Mech.* **1972**, *51*, 3−5.

(23) Plummer, L. N.; Busenberg, E. The solubilities of calcite, aragonite and vaterite in CO_2−H_2O Solutions between 0 °C and 90 °C, and an evaluation of the Aqueous Model for the System $CaCO_3$−CO_2−H_2O. *Geochim. Cosmochim. Acta* **1982**, *46*, 1011−1040.

(24) Lide, D. E. *CRC Handbook of Chemistry and Physics*; CRC Press: Boca Raton, 2002; Vol. *83*.

(25) Rutte, P. W. M. Diffusion in Liquids. Ph.D. Thesis, Delf University, Delf, The Netherlands, 1992.

(26) Schultz, S. G.; Solomon, A. Determination of the effective hydrodynamic radii of small molecules by viscometry. *J. Gen. Physiol.* **1961**, *44*, 1189−1199.

(27) Krynicki, K.; Green, C. D.; Sawyer, D. W. Pressure and temperature dependence of self-diffusion in water. *Faraday Discuss. Chem. Soc.* **1978**, *66*, 199−208.

(28) Wise, D. L.; Houghton, G. The diffusion coefficients of ten slightly soluble gases in water at 10−60 C. *Chem. Eng. Sci.* **1966**, *21*, 999−1010.

(29) Verhallen, P.; Oomen, L.; Elsen, A.; Kruger, J.; Fortuin, J. The diffusion coefficients of helium, hydrogen, oxygen and nitrogen in water determined from the permeability of a stagnant liquid layer in the quasi-s. *Chem. Eng. Sci.* **1984**, *39*, 1535−1541.

(30) Thomas, W.; Adams, M. Measurement of the diffusion coefficients of carbon dioxide and nitrous oxide in water and aqueous solutions of glycerol. *Trans. Faraday Soc.* **1965**, *61*, 668−673.

(31) Grogan, A.; Pinczewski, W. The role of molecular diffusion processes in tertiary CO_2 flooding. *J. Pet. Technol.* **1987**, *39*, 591−602.

(32) Clarke, J. K. A. Kinetics of absorption of carbon dioxide in monoethanolamine solutions at short contact times. *Ind. Eng. Chem. Fundam.* **1964**, *3*, 239−245.

(33) Tamimi, A.; Rinker, E. B.; Sandall, O. C. Diffusion coefficients for hydrogen sulfide, carbon dioxide, and nitrous oxide in water over the temperature range 293−368 K. *J. Chem. Eng. Data* **1994**, *39*, 330−332.

(34) Unver, A.; Himmelblau, D. Diffusion coefficients of CO_2, C_2H_4, C_3H_6, and C_4H_8 in water from 6° to 65° C. *J. Chem. Eng. Data* **1964**, *9*, 428−431.

(35) Tse, F. C.; Sandall, O. C. Diffusion coefficients for oxygen and carbon dioxide in water at 25 C by unsteady state desorption from a quiescent liquid. *Chem. Eng. Commun.* **1979**, *3*, 147−153.